Appearance Potential of CF_3^+ in the Dissociative Photoionization of CF_3Br

E. A. Walters* and J. T. Clay

Department of Chemistry, University of New Mexico, Albuquerque, New Mexico 87131

J. R. Grover*,†

Department of Chemistry, Brookhaven National Laboratory, Upton, New York 11973

Received: September 13, 2004; In Final Form: December 3, 2004

Measurements of the appearance potential for the production of CF_3^+ in the photoionization of CF_3Br are in sharp disagreement, contributing to controversy in the heat of formation of CF_3^+. We reexamine our previous work and add additional experiments, obtaining $AP(CF_3^+/CF_3Br) = 11.64 \pm 0.04$ eV as the average of four measurements made under widely different conditions. This is higher by 0.08 eV than the value we reported previously. Our new value for $\Delta_f H_0°(CF_3^+)$ is now 88.0 ± 0.9 kcal mol^{-1}. We compare our method with other techniques.

Introduction

Reported measurements of the heats of formation of CF_3 and CF_3^+ show interesting disagreement, with the range from smallest to largest being ∼0.5 eV. This problem has been documented and discussed by many workers.[1−8]

The discrepancy stems in part from measurements of the appearance potential for CF_3^+ from CF_3Br. Noutary[9] and Creasey et al.[10] report 11.84 eV and 11.92 ± 0.02 eV, respectively. Jarvis and Tuckett and Jarvis et al.[1,2] conclude that the probable value of $IP(CF_3)$ is <8.6−8.7 eV, corresponding to $AP(CF_3^+/CF_3Br)$ <11.7−11.8 eV. Asher and Ruscic[3] obtain 12.095 ± 0.005 eV. Garcia et al.[4] report 12.07 ± 0.02 eV. We had reported[11] 11.56 ± 0.02 eV.

The appearance potentials reported in refs 3, 9, and 10 were measured in bulk gas at 300 K, in contrast to the much colder jet-expansion beams used to obviate thermal corrections: CF_3Br/O_2 in ref 11 and CF_3Br/He in ref 4.

Noutary[9] and Asher and Ruscic[3] used laboratory discharge sources of vacuum ultraviolet radiation, the intensities of which are generally 10^{-4}−10^{-3} that of the National Synchrotron Light Source's (NSLS's) beam line U-11, which, with a band-pass of 2 Å, delivers ∼10^{13} photons/s at 11−12 eV. On the other hand, the grating producing monochromatized synchrotron radiation at the NSLS also delivers ∼3×10^{11} photons/s of second-order radiation, an effect not faced with the discharge sources. For refs 3 and 9, targets of ambient gas were roughly comparable in number density to the densities provided by the molecular beams in our experiment. Accordingly, their signal intensities relative to ours must have been crudely proportional to the relative radiation intensities. Thus, Noutary's[9] experiment may not have been able to observe the weak initial onset.

Creasey et al.[10] used synchrotron radiation but did not report photon intensities. They utilized a glass capillary to light-pipe the radiation into their experiment, thus limiting the angular fan of radiation accepted (U-11's fan is 55 mrad). Also, they used coincidence measurements, and for these to be meaningful, the ionization rate must not be too high. Hence, this experiment, also, may have lacked sufficient sensitivity to observe the first onset.

Garcia et al.[4] used synchrotron radiation with a skimmed molecular beam target but with gas-filter and electron−ion coincidence techniques to eliminate second-order radiation. Their sensitivity for weak onsets is unclear.

To analyze their spectra, both Garcia et al. and Asher and Ruscic, who obtained the highest values, employed a formalism[12] in which the data are fitted to a roughly linear trial onset shape convoluted with thermal hot bands, for doing which they used adjustable parameters.

A consensus is growing, guided by the results of the most recent ab initio calculations,[5] that $IP(CF_3)$ is near 9.061 eV, which corresponds to $AP(CF_3^+/CF_3Br)$ being close to 12.1 eV. Reasons suggested in refs 3, 4, and 6 to reject the reported onsets significantly <12.1 eV are the following: (a) misinterpretation of the spectra due to unrelaxed vibrational excitation, (b) beam contamination by thermal molecules, and (c) incorrect threshold analysis.

On the other hand, the lower values of $IP(CF_3)$ and $AP(CF_3^+/CF_3Br)$ receive a surprising amount of support from other methods. In drift-tube experiments, Hansel et al.[8] measured $AP_{300}(CF_3^+/CF_4) \leq 14.28$ eV, from which $AP_0(CF_3^+/CF_3Br) \leq 11.62$ eV. In selected ion flow-tube measurements, Tichy et al.[13] reported $AP_{300}(CF_3^+/CF_4) = 14.2 \pm 0.1$ eV, giving $AP_0(CF_3^+/CF_3Br) = 11.54 \pm 0.1$ eV, and in guided ion beam mass spectrometer measurements, Fisher and Armentrout[14] found $AP_{300}(CF_3^+/CF_4) = 14.24 \pm 0.07$ eV, giving $AP_0(CF_3^+/CF_3Br) = 11.58 \pm 0.07$ eV. These results agree well with each other and are all remarkably consistent with our work. They also support the onsets reported by Noutary and by Creasey et al., when the latter are considered to be upper limits.

Thus, it seemed appropriate to reexamine this problem, both in the light of our published work and to see what change our additional and ancillary measurements would effect.

Experiment

Our experiment is described in sufficient detail to accommodate a discussion of the reasons suggested to explain the discrepancy.

† Present address: 1536 Pinecrest Terrace, Ashland, OR 97520-3427.

10.1021/jp040610b CCC: $30.25
Published on Web 02/04/2005

TABLE 1: Appearance Potential (in eV) for Producing CF_3^+ from CF_3Br under Various Conditions[a]

target gas	AP(CF_3^+/CF_3Br)	P^b	T (K)[c]	AP_{2nd}	AP_{3rd}
$CF_3Br/He = 1.7/98.3$	11.70 ± 0.03	600	3	11.85	12.03
$CF_3Br/O_2 = 0.5/99.5$	11.59 ± 0.03	600	10	11.89	12.07
$CF_3Br/O_2 = 5/95$	11.68 ± 0.03	600	13	11.85	12.06
CF_3Br (neat)	11.58 ± 0.03	100	200	11.90	12.05
averages:	11.64 ± 0.04			11.87	12.05

[a] AP_{2nd} and AP_{3rd} are the second and third onsets, respectively. No attempt was made to correct for hot bands or slip. [b] Nozzle pressure (in Torr). [c] Beam temperature, calculated via eq 3 of ref 22.

System and Conditions. Bromotrifluoromethane was photoionized in a molecular beam crossed at right angles by a beam of tunable vacuum ultraviolet (VUV) radiation, with observation and measurement of the CF_3^+ being produced. Details of the photon and molecular beams are described below.

Photons. The photon beam was provided by the normal incidence Wadsworth monochromator[15] of the U-11 beam line at the 750-MeV electron storage ring of NSLS at Brookhaven National Laboratory. A laminar grating of 1200 lines/mm, configured to suppress second-order radiation[16] at 800 Å, was employed. The photon resolution was 2.3 Å for some experiments and 1.0 Å for others, a function of the monochromator exit slit width. Measurement of the apparent ionization threshold of argon was carried out for each fill of the ring, to adjust for minor changes in the position of the electron beam, which served as the monochromator entrance slit. Most corrections were much less than 1 Å, but one was 1.6 Å in the worst case.

Molecular Beam. The molecular beam targets were formed by the jet expansion of gas mixtures, at the compositions, nozzle temperatures, and pressures indicated in Table 1. Since this work involved high-pressure nozzle discharges into a vacuum system integral with the storage ring vacuum, *rigorous* conditions for ring vacuum integrity demanded that extensive differential pumping be employed. A 10-in. diffusion pump (6000 L s^{-1}) backed by a Roots Blower was used for the nozzle−skimmer region, and separate turbomolecular pumps (500 L s^{-1}) were employed for the skimmer-secondary slit, experimental, and beam-dump volumes. The molecular beam itself was dumped into a helium cryopump, configured to minimize the geometry for backscattering into the experimental chamber of any uncondensed species and maintained at 15 K. Pressure in the experimental volume was $\sim 5 \times 10^{-8}$ Torr with no beam and typically rose to $(1-5) \times 10^{-7}$ Torr (mostly the oxygen or helium diluents) with the beam present. Vacuum was windowless all the way to the NSLS ring and was maintained at sufficiently low background pressures in the monochromator and beam-line to survive exacting facility regulations and unforgiving automatic cutoffs in the event of noncompliance.

The aggressively pumped skimmer-secondary slit section was crucial for minimizing background gas in the experimental region.

For ion detection, a quadrupole mass spectrometer was used, which extracted ions in the direction perpendicular to the molecular beam−photon beam plane, and was operated in the ion-counting mode.

The basic apparatus is diagrammed in ref 17. Significant changes since that paper are the following: (1) the addition of a 500-L s^{-1} turbomolecular pump to the experimental volume, (2) a valve between the skimmer-secondary slit differential-pumping region and the experimental region, (3) temperature control of the nozzle, (4) a window to allow optical monitoring of the nozzle−skimmer relationship, and (5) upstream from the slit, a high-vacuum gate valve bearing an LiF window.

Correction for Second-Order Radiation.[18] The high intensity of synchrotron radiation to as low as 500 Å in the NSLS U-11 monochromator means that a significant intensity of second (and higher)-order radiation appears in the vicinity of most photoion onsets, which are usually in the range 900−1600 Å. The raw photoion production (RPIP) curve of the observed ion generated by this second-order radiation is superimposed upon the first-order RPIP curve and must be removed for accurate determination of the onset. [For the relationship between the RPIP curve and the photoionization efficiency (PIE) curve, see below.] To correct the raw onset RPIP curve, the RPIP curve for the same reaction is also measured at one-half the wavelengths as those in the range within which the onset occurs. Let $S^o(\lambda)$ and $S^c(\lambda)$ be the part of this RPIP curve around the onset and the part at half its wavelengths, respectively. Here, λ is the wavelength calculated from the grating angle as if it were first order, but in the onset region, this radiation is actually a mixture of first-, second-, and third-order components, of wavelengths λ', λ'' ($=^1/_2\lambda'$), and λ''' ($=^1/_3\lambda'$). As long as $\lambda \leq$ 1000 Å, $S^c(\lambda)$ is an essentially pure first-order RPIP curve, that is, $S^c(\lambda) = S^c(\lambda')$, because the mirror and grating strongly absorb wavelengths $\leq$500 Å. At first thought, $S^c(\lambda')$ represents the second-order contribution when plotted at double the wavelength at which it was measured and scaled appropriately could be subtracted from $S^o(\lambda)$ to give the corrected onset RPIP curve. However, $S^c(\lambda')$ plotted thus differs significantly from the requisite second-order RPIP curve, $S^{c''}(\lambda'')$, due to mirror and grating material effects. Hence, we introduce the conversion function $F(\lambda'',\lambda')$, such that

$$S^{c''}(\lambda'') = F(\lambda'',\lambda')\, S^c(\lambda') \tag{1a}$$

Since $S^c(\lambda')$ and $S^{c''}(\lambda'')$ are proportional to the first- and second-order radiation intensities, $I'(\lambda')$ and $I''(\lambda'')$, we have

$$F(\lambda'',\lambda') = I''(\lambda'')/I'(\lambda') \tag{1b}$$

evaluated at $\lambda'' = \lambda'$. When λ' is in the range of half the wavelength of the onset, λ'' occurs directly in the range of the onset. Subtraction of $S^{c''}(\lambda'')$ from the raw onset RPIP curve, $S^o(\lambda)$, then leaves the onset RPIP curve, $S^o(\lambda')$, due only to the first-order radiation

$$S^o(\lambda') = S^o(\lambda) - NS^{c''}(\lambda'') \tag{2}$$

where N is a normalizing constant whose value makes the product $NS^{c''}(\lambda'')$ match $S^o(\lambda)$ at values of λ greater than the observed onset. The relative cross section, $\sigma(\lambda')$ (i.e., the PIE curve), is then

$$\sigma(\lambda') \propto S^o(\lambda')/I'(\lambda') \tag{3}$$

The ratio of radiation intensities, $I''(\lambda')/I'(\lambda')$, was measured as follows. Since these intensities are directly proportional to the corresponding ion yields, $F(\lambda'',\lambda')$ may be constructed from the yield curves of reactions with distinct onsets in the range of the wavelength span of interest. Seven such reactions, $i = 1-7$, were utilized.[20] One of these is illustrated in Figure 1. After small corrections for higher-order contributions, the ratio of second-order signal at a specific wavelength, $S^{i''}(\lambda'')$, divided by the corresponding first-order signal, $S^{i'}(\lambda')$, gives the apparatus function, $F_i(\lambda'',\lambda')$, for this reaction.

$$F_i(\lambda'',\lambda') = S^{i''}(\lambda'')/S^{i'}(\lambda') = [I''(\lambda'')/I'(\lambda')]_i \tag{4}$$

The experimentally measured functions, $[I''(\lambda'')/I'(\lambda')]_i$, were

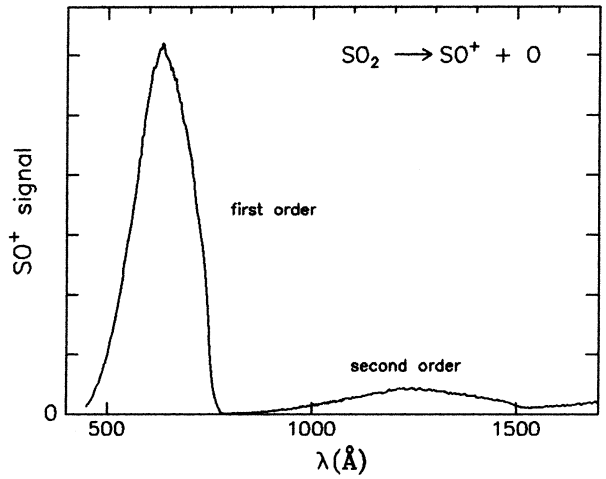

Figure 1. Signal of SO^+ observed for a beam of SO_2 expanded neat at a nozzle pressure of 990 Torr and a resolution of 2.3 Å. The value of λ is calculated from the grating angle as if it were first order. Above 1600 Å, the signal rises toward the third-order peak.

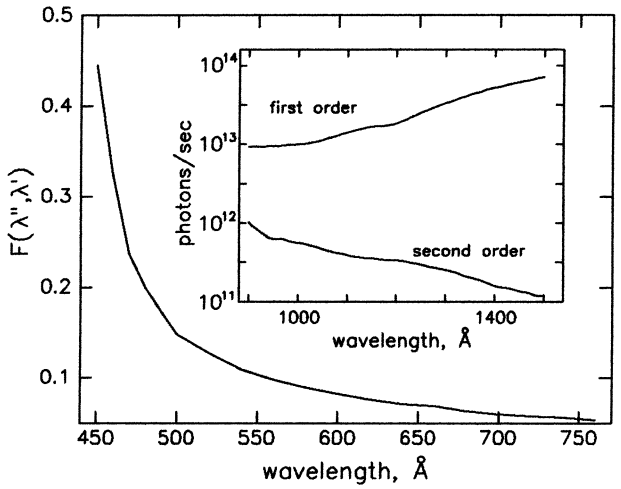

Figure 2. Wavelength dependence of the ratio of second-order ion intensity to first-order ion intensity, $F(\lambda'',\lambda')$, where grating settings are such that $\lambda' = \lambda''$. Inset: comparison of the first-order and second-order light intensities for a 2-Å band-pass and ring current of 500 mA, and at the grating angles for λ'. Here, we make use of the virtual wavelength independence for counting scintillations from fresh sodium salicylate surfaces.[21]

combined and averaged to assemble the needed apparatus function, $F(\lambda'',\lambda')$, over the entire region of interest. All seven measurements were in excellent agreement.

Figure 2 gives the average $F(\lambda'',\lambda')$ from these studies, while the inset presents typical intensities of first- and second-order radiations at given grating angles. Once the function $F(\lambda'',\lambda')$ has been determined over a wide range of wavelengths, the product $F(\lambda'',\lambda')\ S^c(\lambda')$ is readily evaluated as needed.

Result

Figure 3 shows the raw data (points) and the separately measured second-order background (line) for the 0.5/99.5 CF_3Br/O_2 mixture. The onset is close to 11.6 eV. Here, the signal intensity around the minimum was ~2800 counts/(point•s), for a nozzle pressure of 600 Torr, a band-pass of 2.3 Å, and a ring current of 290 mA. This measurement, plus the ancillary measurement to determine the second-order correction, required ~25 min to perform. In Figure 4, the second-order contribution has been subtracted to facilitate determination of the appearance potential, $AP(CF_3^+/CF_3Br) = 11.59$ eV.

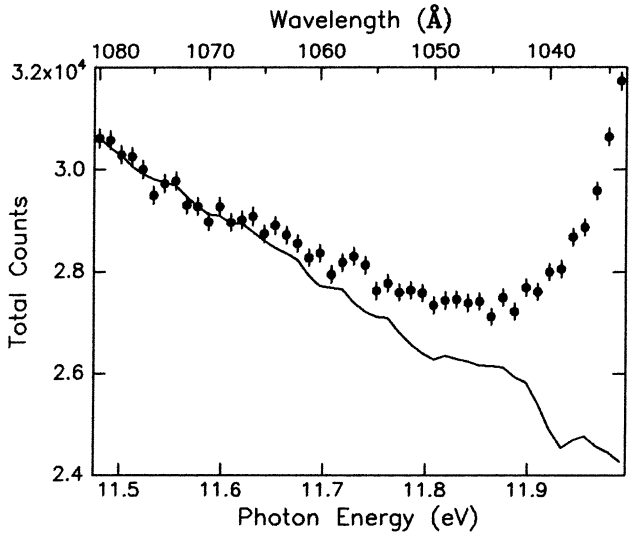

Figure 3. Expanded view of raw counts of CF_3^+ (points) and separately measured background due to second-order radiation (line). Expansion conditions: 199/1 O_2/CF_3Br at a nozzle temperature and pressure of 296 K and 600 Torr, respectively. The error bars show one sigma of uncertainty from the number of counts. The corresponding uncertainties of the second-order counts, not shown, are one-third as large.

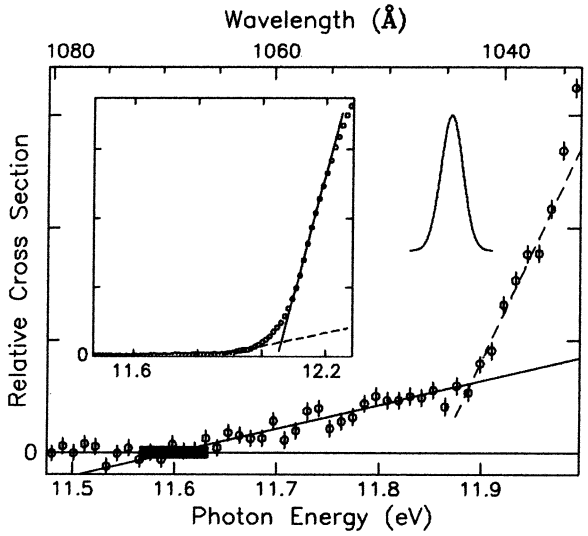

Figure 4. Net yield per photon of CF_3^+ from CF_3Br (points) for the data of Figure 3. The vertical line at each point shows one sigma of uncertainty due to the statistics of counting, including the contribution from the second-order background. The solid straight line is the least-squares fit for the first onset, where the black rectangle about the intercept indicates the 68% confidence region of the appearance potential. The dashed straight line is a least-squares fit for the second onset. Inset: the points are the data, the solid line is a straight-line fit about the inflection, and the dashed line is a least-squares fit for the second onset. Inset curve: instrumental resolution.

Table 1 lists the appearance potential observed for four different conditions. All the APs agree well with each other, with the average being 11.64 ± 0.04 eV, where the range represents the 68% confidence level.

Table 1 also gives the two apparent onsets at successively higher energies, AP_{2nd} and AP_{3rd}, with their simple average values being 11.87 and 12.05 eV, respectively. AP_{2nd} was determined by the intercept with the line used to determine AP_{1st} of a second reasonably well-fitted straight line, shown dashed in Figure 4. However, AP_{3rd}, by far the most intense, was determined as the intercept of the straight line fitted about the inflection point of the data, with the line used to determine

AP_{2nd}. This is depicted for the 0.5/99.5 CF_3Br/O_2 mixture in the upper left inset of Figure 4. We identify AP_{3rd} with the appearance potentials reported in refs 3 and 4.

The onsets of 11.84 and 11.92 eV reported by Noutary[9] and Creasey et al.[10] agree well with AP_{2nd}, indicating that their experiments were not sensitive enough to observe the weak first onset. On the other hand, such close agreement gives strong support to the present work.

The reported measurements of $AP(CF_3^+/CF_3Br)$ fall into two categories, those measured via monochromatized synchrotron radiation, that is, intense sources contaminated by second-order radiation, and those measured via significantly weaker sources, namely, second-order-free discharge sources or synchrotron radiation from which second-order contamination has been removed. Thus, there is a standoff between data that, although free of the contribution from second-order radiation, are of too low intensity to show a weak onset ramp easily and data that, although more intense, from which the contribution caused by second-order radiation must be subtracted, so that the onset region is comprised of the small difference between large intensities.

Above the linear portion of the AP_{2nd} intercept, the data curve sharply upward (see Figure 4), in what has been interpreted as a hot band of what we have reported as the AP_{3rd} onset. Since this feature is still present, and essentially unchanged, for beam temperatures of 3−13 K, it cannot be entirely a hot band. It is reasonably explained as containing an unresolved series of rovibrational onsets of CF_3^+. However, this leaves unexplained the apparent absence of onsets between 11.64 and 11.87 eV, a region 1500−2300 cm^{-1} wide, within which vibrational levels of CF_3^+ also exist.

Discussion

Possible Sources of Error. *Hot Bands.* The presence of hot bands due to unrecognized high beam temperature was cited as a possible contributing factor for the underestimation of onset energies. In our experiments, terminal beam temperatures were estimated from the equation[22]

$$T_B = T_0[1 + 4.8 \times 10^4(\gamma - 1)^5(P_0D)^{2(\gamma-1)/\gamma}]^{-1}$$

using $\gamma = 1.136$ for CF_3Br,[23] $\gamma = 1.396$ for O_2,[24] and $\gamma = 1.660$ for He.[24] [T_0 and P_0 are the temperature (K) and pressure (atm) of the source gas, respectively, D is the nozzle diameter (cm), and $\gamma = C_p/C_v$ is the source gas heat capacity ratio.] Temperatures calculated from this equation are consistent with observations in various laboratories (see ref 22). For a recent kinetic energy release beam temperature measurement of 5 K for jet expansions of 10% pentane/90% argon, measured in Baer's laboratory,[25] the above expression gives ∼10 K. This and other recent cases suggest that the expression may overestimate beam temperatures in the region of a few degrees K.

The PIE spectra of the various products arising from the photoionization and dissociative photoionization of CF_3Br do not have onsets sharp enough to allow direct estimates of beam temperature. Therefore, we carried out ancillary experiments on a system quite similar to that used to measure $AP(CF_3^+/CF_3Br)$, from which the beam temperature was estimated to be ≤30 K.[26] To do this, we utilized the sharp onset spectrum of C_6F_6. The onset spectrum from the photoionization of 1/110 C_6F_6/O_2 expanded at 1000 Torr, under conditions comparable to our CF_3Br/O_2 work, was contrasted with the thermal (296 K) photoionization spectrum of C_6F_6, obtained with 1×10^{-6} Torr of C_6F_6 ambient in the photoionization chamber. We carried out several runs in which we alternated between beam and thermal conditions, to be sure that the two data sets were at the same resolution. An LiF filter eliminated second-order radiation (and also isolated the experimental chamber from the ring vacuum). As depicted in Figure 5, the intercept for the cold beam was linear and abrupt, which was the reason for picking this system. On the other hand, the thermal spectrum for C_6F_6 displayed an appreciable hot-band curved foot or "tail". The least-squares intercept for the nozzle beam is 9.905 eV. The thermal intercept, based on a least-squares fit to the linear portion just above the foot, is 9.885 eV. Thus, there is a significant contribution from hot bands in the thermal spectrum, enough to demonstrate that there is very little room-temperature C_6F_6 present in the nozzle beam and that, in fact, the latter is quite cold. The beam temperature was estimated from this comparison to be $T_B \leq 30$ K and was calculated from the above-cited equation to be ∼10 K. Due to its high symmetry, one expects C_6F_6 to be more difficult to cool in a jet expansion than CF_3Br would be.

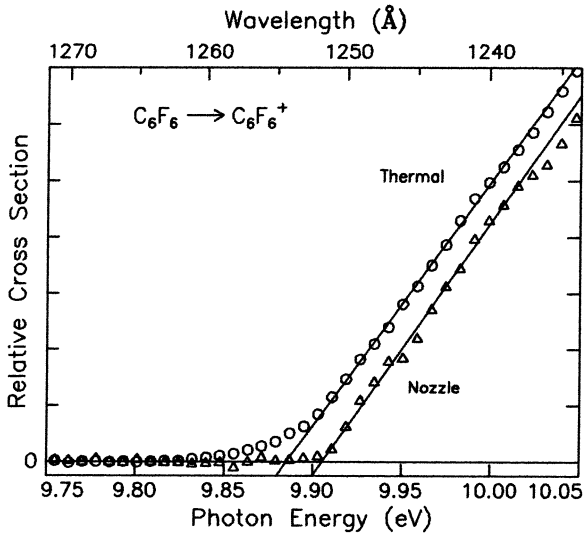

Figure 5. Comparison of the production of $C_6F_6^+$ from C_6F_6 from thermal background gas at 296 K, with production in a beam formed from jet expansion of the gas mixture 110/1 O_2/C_6F_6 at 1000 Torr of nozzle pressure.

The room-temperature photoelectron spectrum of C_6F_6, measured by Bastide et al.,[27] might afford an opportunity to verify the presence of hot bands. Indeed, a detailed examination of their data reveals that their onset spectrum tails down to 9.6 eV. The first peak in the vibrational progression is at 9.90 eV, taken by those authors to be the adiabatic IP, in excellent agreement with our nozzle intercept. However, they specify their resolution to be 0.07 eV, which is consistent with the tailing. Thus, comparison with our measurements in Figure 5, in which the hot bands cause a displacement of only 0.02 eV, shows that the Bastide et al. work was not sensitive enough to support our observation.

Thermal Molecules Polluting the Beam. It is sometimes asserted that nozzle expansions are always polluted with a large proportion of thermally unrelaxed molecules, for which misapprehension of a paper from Baer's laboratory[28] may be cited but misunderstood. Indeed, it is well-known that vibrational cooling can be inefficient for jet expansions of certain neat gases, for example, nitrogen. However, as far as we are aware, this phenomenon occurs only in special cases and is mitigated or eliminated in mixtures that allow efficient relaxation of vibrational energy.

The lack of thermal contamination in our apparatus can be seen in the nozzle expansion of C_6F_6/O_2 to produce the spectrum

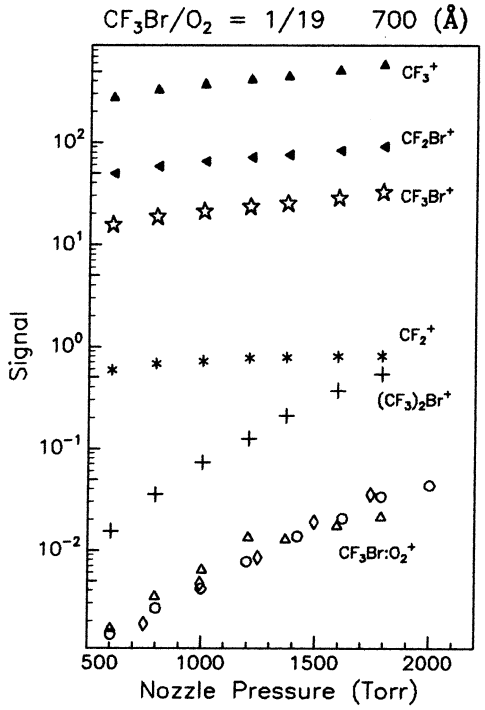

Figure 6. Pressure-dependent inventory of ions produced by photoionization of a beam formed by jet expansion of the mixture 1/19 CF_3Br/O_2 at a wavelength of 700 Å.

of Figure 5. Here, the production of $C_6F_6 \cdot O_2$ is far advanced (see Figure 1c of ref 29) to the point that production of trimers is showing up, because just above this pressure the curve begins to round off due to the competitive production of trimers (and larger clusters). This is strong evidence that the amount of vibrational energy stored in monomer C_6F_6 must be very small, particularly since one expects clusters to be at somewhat higher temperatures than the bath gas. In further support of unblurred onsets as evidence of low temperatures, we note that the dissociation energy of $C_6H_6 \cdot O_2$ (measured under comparable conditions in the same project), via the onset of $C_6H_6^+$ from $C_6H_6 \cdot O_2$, was recently verified to good accuracy in a different type of experiment, carried out by Casero and Joens.[30]

Direct evidence was observed in kinetic energy release (KER) measurements,[31] where contamination by thermal molecules was demonstrated to be <1% for He/Ar mixtures, illustrated for 19/1 He/Ar in Figure 3a of ref 31. Furthermore, the traces of thermal contamination seen in the KER experiments were much larger than would be true for the work being reported here, because the KER work incorporated an extra slit inside the experimental chamber that scattered 93% of the molecular beam entering the chamber, which would otherwise have been captured by the beam dump.

As additional evidence for the CF_3Br/O_2 system being discussed here, the complexes $CF_3Br \cdot O_2$ and $(CF_3Br)_2$ [seen via $(CF_3)_2Br^+$] were being produced under the same conditions in which we measured the onset of CF_3^+ (see Figure 6). This is compelling evidence for low temperatures and a lack of pollution by hot molecules, especially because oxygen complexes are so weak ($D_0 \sim 2$ kcal mol^{-1}). It is unreasonable that these complexes could exist at the same time that a large proportion of the bath molecules are vibrationally excited at room temperature. Thus, the existence of fragile van der Waals (vdW) complexes in proportions far larger than what would occur at equilibrium near 300 K provides a stringent constraint on the proportion of thermally hot molecules that can be present.

For the CF_3Br/O_2 mixtures, it is unlikely that CF_3Br fails to relax in the expansion, for its complement of vibrational modes is not such that $V \rightarrow T,R$ processes should have low probability. One can point especially to the bend and stretch involving Br (306 and 349 cm^{-1}), and to the CF_3 deformations (547 and 760 cm^{-1}).[32] On mechanical grounds, we would expect these motions, which constitute nearly all of the vibrational excitation (96.7%) in the 296 K species going into the expansion, to be readily coupled to translation in collisions with the bath-gas molecules of O_2, which are nonspherical and of considerable mass. In any case, the experiments using oxygen were carried out at high dilution, namely, $CF_3Br/O_2 = 5/95$ and 0.5/99.5. For the mixture CF_3Br/He, the deexcitation by He would be more difficult because of helium's low mass. Deexcitation in the neat beam could be incomplete, although this would not be so clear because the beam temperature is expected to be relatively high, ~200 K.

As for the often-misunderstood Baer work cited above, Baer explained in his paper that his 25% of signal due to uncooled molecules was due to ambient background, *not* inefficient jet-expansion cooling.[28] We therefore reexamined our data for ambient background. It had to be low, because our apparatus demanded aggressive pumping, as described above. Background spectra measured at the time of our experiment indicated a mass 69 contribution from ambient gas, S_{69}, of ≪4 counts/(s·100 mA of ring current), several orders of magnitude less than the CF_3^+-counting levels in the experiments. This limit comes from background measurements that average <4 counts/(s·100 mA) at 584 Å, falling to <0.7 counts/(s·100 mA) at 1080 Å. For the data displayed in Figure 3, it means the background level is ≪100 total counts, where the counting uncertainty is ~170 counts.

Underestimation of AP(CF_3^+/CF_3Br). Several effects, considered below, could cause an AP to be apparently too low: (1) an impurity, (2) interference by van der Waals clusters, (3) Rydberg states, (4) metastable states, and (5) kinetic shift.

(1) An impurity, especially CF_3I. Extensive inventory scans at 700 Å found no impurities of the kind, or in amounts, that could interfere. In particular, CF_3I could not be detected. If present, it would be at a level of $<10^{-5}$ of the CF_3Br.

(2) The observed onset of CF_3^+ is for a van der Waals dimer, either $CF_3Br \cdot O_2$ or $(CF_3Br)_2$.

$$CF_3Br \cdot O_2 + h\nu \rightarrow CF_3^+ + BrO_2 + e^- \qquad \text{(A)}$$

$$(CF_3Br)_2 + h\nu \rightarrow CF_3^+ + CF_3Br_2 + e^- \qquad \text{(B)}$$

Reaction A: If indeed AP(CF_3^+/CF_3Br) = 12.095 eV, then the onset of 11.64 eV would give $\Delta_f H_0°(BrO_2) = 16$ kcal mol^{-1}. This value results from using $\Delta_f H_0°(CF_3Br \cdot O_2) = -154.2$ kcal mol^{-1}, where it is assumed that $D_0(CF_3Br \cdot O_2) = 2$ kcal mol^{-1}, in agreement with the values of van der Waals binding[33] of O_2 to similar substrates, and using the tabulated value[34] $\Delta_f H_0°(CF_3Br) = -152.2$ kcal mol^{-1}. The value 16 kcal mol^{-1} is much smaller than the known value,[35] $\Delta_f H_0°(OBrO) = 41.4 \pm 1.0$ kcal mol^{-1}. The threshold for reaction A should therefore be 12.75 eV (or 12.30 eV for an onset of 11.64 eV) and cause no interference.

On the other hand, one might consider the van der Waals species $Br \cdot O_2$ as a possible product. If $D_0(Br \cdot O_2) = 2$ kcal mol^{-1}, as also assumed for $D_0(CF_3Br \cdot O_2)$, then AP($CF_3^+/CF_3Br \cdot O_2$) would be the same as for AP(CF_3^+/CF_3Br), or the two APs would differ only by the small difference between the two van der Waals bindings, which would be of the order 1 kcal mol^{-1} or 0.05 eV.

Reaction B: If AP(CF_3^+/CF_3Br) = 12.095 eV, then the onset of 11.64 eV would give $\Delta_f H_0°(CF_3Br_2) = -137$ kcal mol^{-1}. Here, we estimate $\Delta_f H_0°(CF_3Br)_2 = -306.4$ kcal mol^{-1}, assuming that $D_0(CF_3Br{\cdot}CF_3Br) = 2$ kcal mol^{-1}, the order of van der Waals binding to be expected. The value -137 kcal mol^{-1} would give a stable pentavalent carbon, that is, where $D_0(CF_3Br-Br) = 12$ kcal mol^{-1}. To the authors' knowledge, pentavalent carbon compounds are unknown and probably can only exist in metastable forms (see the discussion in ref 36 and the description of the metastable molecule ND_4 in ref 37).

With the van der Waals species $CF_3Br{\cdot}Br$ as a possible product, using $D_0(CF_3Br{\cdot}Br) = 2$ kcal mol^{-1}, then AP(CF_3^+/[$CF_3Br{\cdot}CF_3Br$]) and AP(CF_3^+/CF_3Br) would differ only by the small difference between the two van der Waals bindings, as already discussed above for AP($CF_3^+/CF_3Br{\cdot}O_2$).

Thus, interference by either reaction A or reaction B, aside from the possible slight blurring described above, is therefore rejected. However, even this blurring problem is unlikely because, at the nozzle pressure used for our measurement, 600 Torr, the signal intensities of $(CF_3Br)_2^+$ and $(CF_3Br{\cdot}O_2)^+$ are 3 and 4 orders of magnitude, respectively, smaller than the intensity of CF_3Br^+, as shown in Figure 6, indicating that the concentrations of the neutral van der Waals complexes are very small compared to the CF_3Br target.

(3) Field-induced dissociative ionization from high Rydberg states. The effect is too small, of the order 0.002 eV, for the draw-out fields of 20−40 V cm^{-1} that we use. See, for example, the calculation of this effect presented in ref 38.

(4) The presence of a metastable state(s). There was no mechanism to excite such a state, and no candidate state is known to the authors.

(5) Kinetic shift.[39,40] It cannot have a serious effect here because the dissociation energy of $CF_3Br^+ \rightarrow CF_3^+ + Br$ is quite low (6 kcal mol^{-1} according to this work but still only 15 kcal mol^{-1} according to a heat of formation of $\Delta_f H_0°(CF_3^+) =$ 98.1 kcal mol^{-1}). For example, see the calculations given in ref 41, which show that the kinetic shift for a dissociation energy of 15 kcal mol^{-1} is negligible for the breakup of even a 16-atom complex.

In summary, we reject all of the above effects.

Comparison of the Observed Spectra with Thermal Hot Bands. The similarity of the low-energy portion of our spectrum to the regions interpreted in refs 3 and 4 as due only to the presence of thermal hot bands is unexpected, if their interpretation is correct, in view of the differing techniques used in the experiments. Therefore, we compared our onset region with those of refs 3 and 4 and with the linear-kernel prethreshold expression given in the appendix of ref 12, assuming an onset of 12.095 eV.[3] For this calculation, we applied the normal modes for CF_3Br listed by Shimanouchi[32] to the Whitten−Rabinovich vibrational level density prescription[42] (i.e., a harmonic approximation), extended to include rotational levels using the moments of inertia of the ground-state structure: in Herzberg's notation,[36] $A_0 = 0.1877$ cm^{-1} and $B_0 = 0.0696$ cm^{-1}.

The comparison is shown in Figure 7. The plot is logarithmic to emphasize the onset region. The open diamonds are read at intervals of 0.02 eV from the data reported in Figure 6 of ref 3, and the closed triangles are the data points given in Figure 4 of ref 4. The diamonds are plotted with an arbitrary displacement for ease of comparison. The data of our work are plotted as open circles, with error bars representing one sigma of uncertainty, based on the statistics of counting. The calculation is given by the solid line, arbitrarily normalized to our data at 12.05 eV.

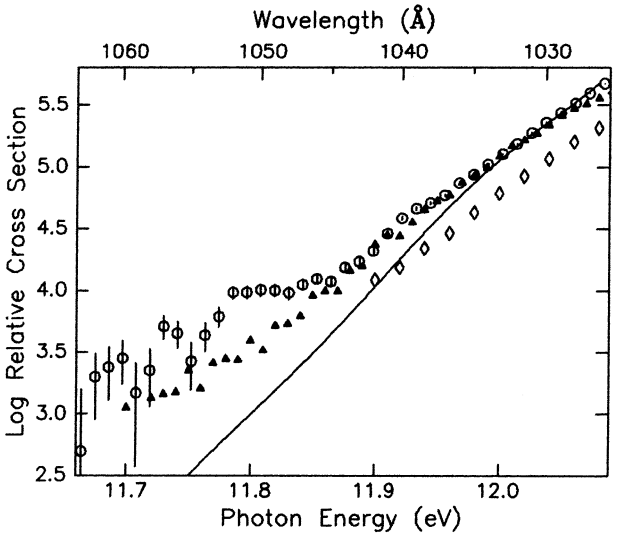

Figure 7. Semilog-scale comparison of the data of this work (combined data of 0.5/99.5 and 5/95 CF_3Br/O_2, open circles) with those of refs 3 (open diamonds) and 4 (closed triangles) and with the theoretical fit of ref 12 (solid line) assuming an onset of 12.095 eV and a target temperature of 300 K.

All three data sets coincide until the energy falls to 11.9 eV. This is despite their origin from different experimental methods, an indication contrary to what one expects from simple thermal bands. Below ~11.8 eV, our data are higher than the data of ref 4, by a factor of 2−3.

The calculated line representing the 300 K hot band follows all three experiments down to 12.0 eV but then falls farther and farther below the data, by more than an order of magnitude at 11.7 eV. The pronounced wavelike structure in our data is due to the onsets at 11.64 and 11.87 eV.

The match of slopes above 12.0 eV for the expansion-cooled and thermal data is coincidental. Even if it is not, for example, if it is due to an unexpectedly large thermal component, the lower onsets of our data and those of ref 4 cannot be explained with thermal contamination at only 300 K. A much higher temperature would be required. It would be interesting to include the data of ref 3 in this comparison, but we could not read its plots below 11.90 eV.

The demand of the analysis of ref 12, that its suggested analysis function, via adjustable parameters, match the low-energy portion of the spectrum, risks overlooking weak spectral contributions at lower energy. It would be interesting to test the data of refs 3 and 4 to see to what extent a more complex kernel can be justified, for example, by the appropriate application of chi-square tests.

One might consider a threshold analysis via quasi-equilibrium theory (QET) calculations. However, such an effort would be hampered by the presently incomplete knowledge of the initial and final states involved. Also, there may be prompt competition between ionization and dissociation into neutrals, and, for the freshly populated ionic states, between immediate dissociation and intramolecular relaxation into slowly dissociating species. It is not obvious to us that there would always be 100% ionization, or 100% slow dissociation.

Possible Effect of Spin−Orbit Splitting in Product Br. For the process $CF_3Br^+ + h\nu \rightarrow CF_3^+ + Br + e$, the weak onset at 11.64 eV and the strong onset at 12.095 eV (or our 12.05 eV) are separated by 0.455 ± 0.04 eV (or 0.41 ± 0.04 eV), the same as bromine's spin−orbit splitting of 0.456 eV. In addition, if the dissociation of excited CF_3Br^+ to give $Br(^2P_{1/2})$ is much more facile than that to give $Br(^2P_{3/2})$, in analogy to behavior[43]

observed for CF_3I^+, the adiabatic appearance potential could be difficult to see with thermal hot bands present. Thus, the relative sensitivity of the various experiments becomes important.

The possible significance of previous observations of the inhibited dissociation of CF_3X^+ to produce ground-state $X(^2P_{3/2})$, in contrast to facile dissociation to form $X(^2P_{1/2})$, is downplayed in ref 3. However, for CF_3Cl^+, a tail contribution above what can be easily explained as thermal is reported in ref 3. This tail provides evidence that there could be production of $Cl(^2P_{3/2})$ underneath the hot bands associated with producing $Cl(^2P_{1/2})$.

Possible Interference of Barriers in $AP(CF_3^+/C_2F_4)$ and $AP(CF^+/C_2F_4)$. The strongest evidence against the lower heat of formation of CF_3^+ stems from measurements[3] of $AP(CF_3^+/C_2F_4)$ and $AP(CF^+/C_2F_4)$. However, recent comments by Jarvis and Tuckett[1] call attention to the possibility of a barrier in these dissociative ionizations, which involve fluorine atom transfer, and may therefore involve an activation energy.

An unremarked problem is that the reported[3] AP values 13.721 and 13.777 eV are almost coincident with the intense autoionizing Rydberg resonance at 13.75 eV,[33,44] which dominates the photoionization spectrum of C_2F_4. This pronounced peak could so enhance an above-adiabatic onset or, alternatively, so distort the shape of an above-adiabatic onset, as to hide a weak adiabatic threshold under its thermal distribution.

Summary

We report measurements of $AP(CF_3^+/CF_3Br)$ to help resolve the 0.5-eV disagreement among several workers, which ranges from 11.56 to 12.095 eV. This disparity contributes to the 0.5-eV uncertainty in $\Delta_f H_0°(CF_3^+)$ that also includes inconsistencies from other kinds of experiments. Our average of four photoionization thresholds, made under widely different conditions, is $AP(CF_3^+/CF_3Br) = 11.64 \pm 0.04$ eV, a value remarkably consistent with several quite different experiments. We describe our experiment in sufficient detail to discuss and reject criticisms of our threshold determinations of the production of CF_3^+ from CF_3Br. In particular, our cold molecular beam targets obviate corrections for hot bands, while the intense synchrotron radiation at line U-11 at Brookhaven's National Synchrotron Light Source provides the sensitivity to observe an onset at lower energy than previously reported. The crucial correction for second-order radiation is described in detail. Rigorous vacuum maintenance eliminated interference from background gas. Several other possible objections are examined and rejected.

Acknowledgment. This research was carried out at Brookhaven National Laboratory under contract DE-AC02-76CH00016 with the U.S. Department of Energy and supported by its Division of Chemical Sciences, Office of Basic Energy Sciences.

References and Notes

(1) Jarvis, G. K.; Tuckett, R. P. *Chem. Phys. Lett.* **1998**, *295*, 145−151.
(2) Jarvis, G. K.; Boyle, K. J.; Mayhew, C. A.; Tuckett, R. P. *J. Phys. Chem. A* **1998**, *102*, 3219−3229.
(3) Asher, R. L.; Ruscic, B. *J. Chem. Phys.* **1997**, *106*, 210−221.
(4) Garcia, G. A.; Guyon, P.-M.; Powis, I. *J. Phys. Chem. A* **2001**, *105*, 8296−8301.
(5) Botschwina, P.; Horn, M.; Oswald, R.; Schmatz, S. *J. Electron Spectrosc. Relat. Phenom.* **2000**, *108*, 109−122.
(6) Irikura, K. K. *J. Am. Chem. Soc.* **1999**, *121*, 7689−7695.
(7) Horn, M.; Oswald, M.; Oswald, R.; Botschwina, P. *Ber. Bunsen-Ges. Phys. Chem.* **1995**, *99*, 323−331.
(8) Hansel, A.; Scheiring, Ch.; Glantschnig, M.; Lindinger, W.; Ferguson, E. E. *J. Chem. Phys.* **1998**, *109*, 1748−1750.
(9) Noutary, C. J. *J. Res. Natl. Bur. Stand. (U.S.)* **1968**, *72A*, 479−485.
(10) Creasey, J. C.; Smith, D. M.; Tuckett, R. P.; Yoxall, K. R.; Codling, K.; Hatherly, P. A. *J. Phys. Chem.* **1996**, *100*, 4350−4360.
(11) Clay, J. T.; Walters, E. A.; Grover, J. R.; Willcox, M. V. *J. Chem. Phys.* **1994**, *101*, 2069−2080.
(12) Asher, R. L.; Appelman, E. H.; Ruscic, B. *J. Chem. Phys.* **1996**, *105*, 9871−9795.
(13) Tichy, M.; Javahery, G.; Twiddy, N. D.; Ferguson, E. E. *Int. J. Mass Spectrom. Ion Processes* **1987**, *79*, 231−235.
(14) Fisher, E. R.; Armentrout, P. B. *Int. J. Mass Spectrom. Ion Processes* **1990**, *101*, R1.
(15) Howells, M. R. *Nucl. Instrum. Methods* **1982**, *195*, 215−222.
(16) Franks, A.; Lindsey, K.; Bennett, J. M.; Speer, R. J.; Turner, D.; Hunt, D. J. *Philos. Trans. R. Soc. London, Ser. A* **1975**, *277*, 503−543.
(17) White, M. G.; Grover, J. R. *J. Chem. Phys.* **1983**, *79*, 4124−4131.
(18) This procedure has been briefly described earlier.[19] We provide a more complete description here.
(19) Walters, E. A.; Grover, J. R.; White, M. G. *Z. Phys. D* **1986**, *4*, 103−110.
(20) Higher-order spectra utilized: He^+ from He, $C_2H_4Cl^+$ and $(C_2H_4{\cdot}HCl)^+$ from C_2H_4/HCl, $C_6H_5^+$ and $C_6H_6^+$ from C_6H_6/He, Ar^+ from Ar, and SO^+ from SO_2.
(21) Samson, J. A. R. *Techniques of Vacuum Ultraviolet Spectroscopy*; John Wiley & Sons: New York, 1967; pp 214−215. No attempt was made to correct for the slight wavelength dependence of the detection efficiency between 1250 and 1600 Å.
(22) Grover, J. R.; Walters, E. A.; Newman, J. K.; White, M. G. *J. Am. Chem. Soc.* **1985**, *107*, 7329−7339.
(23) Calculated from $C_p° = 16.6$ cal/g·mol for CF_3Br at 300 K, where $C_p°$ was calculated from the normal modes tabulated in ref 32.
(24) Calculated from $C_p° = 7.0$ cal/g·mol for O_2 and $C_p° = 5.0$ cal/g·atom for He, at 300 K, as tabulated in Benson, S. W. *Thermochemical Kinetics*; John Wiley & Sons: New York, 1976; p 289.
(25) Riley J. S.; Baer, T. *Int. J. Mass Spectrom. Ion Processes* **1994**, *131*, 295−305.
(26) Due to a typographical error, the beam temperature, cited as 30 K in ref 11, should have read ≤30 K.
(27) Bastide, J.; Hall, D.; Heilbronner, E.; Maier, J. P.; Plevey, R. G. *J. Electron Spectrosc. Relat. Phenom.* **1979**, *16*, 205−208.
(28) Weitzel, K.-M.; Booze, J. A.; Baer, T. *Chem. Phys.* **1991**, *150*, 263−273.
(29) Grover, J. R.; Hagenow, G.; Walters, E. A. *J. Chem. Phys.* **1992**, *97*, 628−642.
(30) Casero, J. J.; Joens, J. A. *J. Phys. Chem.* **1997**, *101*, 2607−2609.
(31) Grover, J. R.; Walters, E. A.; Arneberg, D. L.; Cheng, B.-M.; Hagenow, G.; Clay, J. T.; Willcox, M. V. Manuscript submitted for publication, 2005.
(32) Shimanouchi, T. *J. Phys. Chem. Ref. Data* **1977**, *6*, 993−1102.
(33) Cheng, B.-M.; Preses, J. M.; Grover, J. R. *J. Chem. Phys.* **1997**, *106*, 6698−6708.
(34) Lias, S. G.; Bartmess, J. E.; Liebman, J. F.; Holmes, J. L.; Levin, R. D.; Mallard, W. G. *J. Phys. Chem. Ref. Data* **1988**, *17* (Suppl. 1), 1−861.
(35) Klemm, R. B.; Thorn, R. P., Jr.; Stief, L. J.; Buckley, T. J.; Johnson, R. D. *J. Phys. Chem. A* **2001**, *105*, 1638−1642.
(36) Herzberg, G. *Molecular Spectra and Molecular Structure. III. Electronic Spectra and Electronic Structure of Polyatomic Molecules*; Krieger: Malabar, FL, 1991 (reprint edition with corrections and updates).
(37) Watson, J. K. G. *J. Mol. Spectrosc.* **1984**, *107*, 124−132.
(38) Grover, J. R.; Walters, E. A.; Baumgärtel, H. *J. Phys. Chem.* **1989**, *93*, 7534−7535.
(39) Friedman, L.; Long, F. A.; Wolfsberg, M. *J. Chem. Phys.* **1957**, *26*, 714−715.
(40) Chupka, W. A. *J. Chem. Phys.* **1959**, *30*, 191−211.
(41) Grover, J. R.; Cheng, B.-M.; Herron, W. J.; Coolbaugh, M. T.; Peifer, W. R.; Garvey, J. F. *J. Phys. Chem.* **1994**, *98*, 7479−7487. See Figure 7 of this paper and the associated discussion.
(42) Whitten, G. Z.; Rabinovitch, B. S. *J. Chem. Phys.* **1963**, *38*, 2466−2473; **1964**, *41*, 1883.
(43) Bombach, R.; D'Annacher, J.; Stadelmann, J.-P.; Vogt, J.; Thorne, L. R.; Beauchamp, J. L. *Chem. Phys.* **1982**, *66*, 403−408.
(44) Grajower, R.; Lifshitz, C. *Isr. J. Chem.* **1968**, *6*, 847−857.